

A HYBRID VOLUME INTEGRAL-FINITE ELEMENTS APPROACH FOR THE SIMULATION OF EDDY CURRENT INSPECTION OF STEAM GENERATOR TUBES IN THE REGION OF QUADRIFOILED SUPPORT PLATE

A. Skarlatos¹, C. Gilles-Pascaud¹, G. Pichenot¹, G. Cattiaux², and T. Sollier²

¹CEA, LIST, F-91191 Gif-sur-Yvette, France

²IRSN, B.P. 17, 92262 Fontenay-aux-Roses, France

ABSTRACT. A hybrid Volume Integral Method (VIM) - Finite Elements Method (FEM) model for the numerical modeling of eddy current inspection of steam generator (SG) tubes near quadrifoiled tube support plates (TSP) is presented. The coupled approach combines the flexibility of the FEM in modeling complex geometries with the numerical efficiency of the VIM, reducing the computational time demanded for the solution of the problem. Material deposit in the TSP openings, responsible for clogging up effects, can also be taken into account with this approach and will be considered in a next stage. The present work is conducted in the context of the further development of the CIVA nondestructive evaluation simulation platform, notably within the undertaken developments concerning coupled FEM-VIM calculations.

Keywords: Tube Support Plates, Finite Elements Method, Volume Integral Method, Hybrid Approach

PACS: 81.70.Ex

INTRODUCTION

The prompt detection of flaws in the tube region near tube support plates (TSP) is of crucial importance for the integrity of steam generators (SG) in pressurized water reactors (PWR) facilities since these particular zones are prone to corrosion and stress corrosion cracking. Efficient theoretical modeling of the eddy current inspection procedures in these zones can therefore be valuable for the assessment of the current techniques and the interpretation of the acquired signals.

The complexity of the TSP usually employed in PWR plants (like those with trefoil and quatrefoil-shaped holes), however, makes the solution of the corresponding eddy current problem a difficult task. Even if these geometries can be properly treated using a finite elements method (FEM) code, it seems preferable in terms of the accuracy and the computational efficiency to apply a coupled volume integral method (VIM) - FEM approach. According to this approach, the primary field is calculated using the FEM for the tube-plate ensemble whereas the flaw response is calculated via the VIM [1,2]. This hybrid technique has already been successfully applied in the simpler case of TSP with circular openings inspected with axial probes [3]. The present contribution deals with the

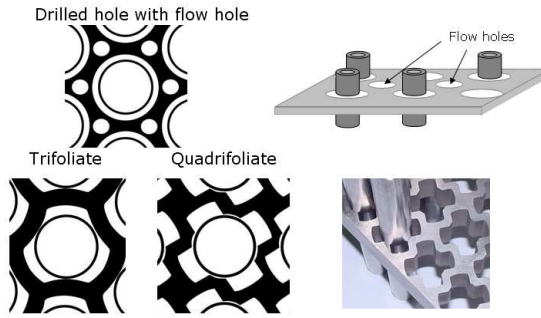


FIGURE 1. Configuration of the TSP used in the steam generators: plate with circular openings, trefoil and quatrefoil plates.

more elaborate case of TSP with trefoil and quatrefoil-shaped holes (cf. Figure 1). The TSP considered here are non-magnetic, although the developed model can also take ferromagnetic plates into account. Ferromagnetic TSPs as well as material deposit effects will be considered in a next step.

This work is done in the framework of a CEA - IRSN collaboration and aims at developing a simulation tool for the inspection of the various parts of industrial SG structures, embedded in the CIVA NDT software platform [4].

THE MODELING APPROACH

The coupling approach adopted in this work is described in [3]. The primary field \vec{E}_2^{inc} , i.e. the electric field induced inside the tube wall in the absence of the flaw, is calculated using the FEM. Since the defect is usually of small volume in respect to the rest of the structure, one can consider that the perturbation to the eddy current flow is of local character and thus neglect its interaction with the TSP. Hence, the flaw response can be calculated with good accuracy by solving the volume integral equation approach applied in the bare tube structure [1, 2]

$$\vec{E}_2(\vec{r}) = \vec{E}_2^{inc}(\vec{r}) + j\omega\mu_0 \int_{V_f} \overline{\overline{\mathbf{G}}}_{22}(\vec{r}, \vec{r}') \delta\sigma(\vec{r}') \vec{E}_2(\vec{r}') dV' \quad (1)$$

where the Green dyad $\overline{\overline{\mathbf{G}}}_{22}$ corresponds to the dyad of a cylindrical multilayered medium. In the above equation, the tube is described in terms of a cylindrical multilayered structure the second layered being assigned to the tube wall, the first and the third ones being referred to the interior and the exterior of the tube respectively. Once the total field \vec{E}_2 has been evaluated, the mutual impedance between the driving coil and each of the receiving coils of the probe can be calculated using the reciprocity theorem [5]:

$$\Delta Z_{ji} = -\frac{1}{I_j I_i} \int_{V_f} \delta\sigma(\vec{r}') \vec{E}_{2,j}^{inc}(\vec{r}') \vec{E}_{2,i}(\vec{r}') dV'. \quad (2)$$

where $\vec{E}_{2,j}^{inc}$ denotes the primary field that would be induced by the considered receiving coil j if it was excited with a current I_j , and I_i is the excitation current of the driving coil. $\vec{E}_{2,i}$ is the total field in the flaw region and is obtained by the solution of Eq. (1). The unperturbed values of the impedance matrix at the different scanning positions Z_{ji} depend on the tube-TSP configuration and are obtained by the post-processing of the FEM solution. The final probe response is then calculated using the above values of Z_{ji} and ΔZ_{ji} taking into account the operational mode of the probe (function in absolute or differential mode).

As in the case of the TSP with circular holes, an optimization algorithm has been developed in order to estimate the most pertinent positions of the probe and hence to minimize the number of FEM simulations.

APPLICATION OF THE HYBRID MODEL FOR THE SIMULATION OF TUBE INSPECTION NEAR A QUATREFOIL TUBE SUPPORT PLATE

The presented model has been applied for the simulation of eddy current inspection of a SG tube in the proximity of a quatrefoil TSP. In order to keep the complexity of the problem restricted, the considered TSP is of stainless-steel (non-magnetic) at this first stage. Ferrous-steel TSPs will be considered in a next step. The results of the hybrid approach have been validated using experimental measurements. The tube and the TSP properties of the experimental mock-up are representative of those met in a typical pressurized water reactor. The mock-up configuration is depicted Figure 2. The tube material is inconel with a conductivity of 1 MS/m and a thickness of 1.27 mm. The conductivity of the TSP was measured at 1.4 MS/m. The probe configuration is shown in Figure 3.

Figure 4 shows the FEM mesh employed for the treatment of the tube-TSP configuration. The FEM calculations are carried out using the Flux-3D package. An important feature of the hybrid approach is that the primary field has to be calculated only once for a given tube, TSP and probe configuration which makes the approach significantly faster than treating the entire problem (primary field and flaw interaction) using the FEM only.

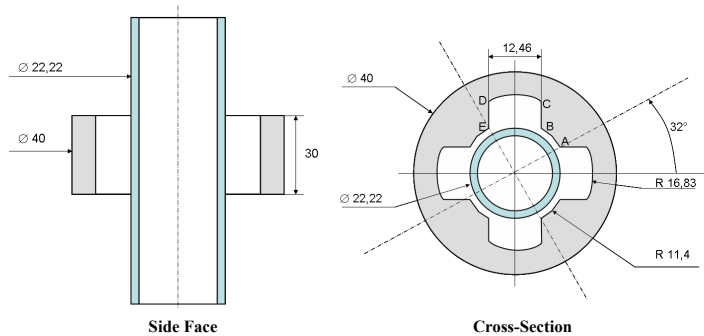


FIGURE 2. Problem configuration: SG tube with a quatrefoil TSP.



2 identical coils operating at differential mode
 Inner radius: 7.83 mm
 Outer radius: 8.5 mm
 Height: 2 mm
 Coils distance: 0.5mm
 Number of turns: 70

FIGURE 3. Problem configuration: SG tube with a quatrefoil TSP.

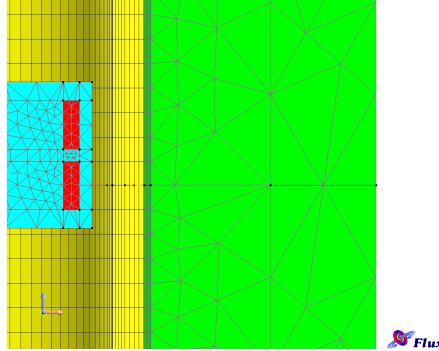


FIGURE 4. Problem configuration: SG tube with a quatrefoil TSP.FEM mesh used for the calculation of the primary field and the self and mutual impedances of the two coils.

The defects considered for the validation of the results are representative of the typical tube degradations in the area of the TSP, which are principally the intergranular stress corrosion cracking (IGSCC). The geometry and the dimensions of the considered flaws are given in Table 1. The EC signals are computed at three frequencies: 100 kHz, 240 kHz and 500 kHz. Both simulation and experimental results are calibrated in respect to the signals of a reference flaw acquired in the absence of the TSP. The reference flaw consists of a set of 4 through-holes of 1 mm diameter, circumferentially distributed every 90°. The amplitude and the phase of the reference signals after the calibration are shown in Table 2.

TABLE 1. Examined flaws for the validation of the developed combined formulation. The flaw radial dimensions are given as percentages of the tube thickness.

Flaw	Dimensions		
	$\Delta\rho/e$	Angular Extension	Longitudinal Extension
External Groove EG40	40 %	360°	1 mm
Transversal Through-Notch TTN82	100 %	82°	0.113 mm
External Longitudinal Notch ELN10	54 %	0.6°	10 mm

TABLE 2. Calibration values at the measuring frequencies.

Frequency	100 KHz	240 KHz	500 KHz
Amplitude	1 V	1.3 V	1 V
Phase	-17°	-30°	-30°

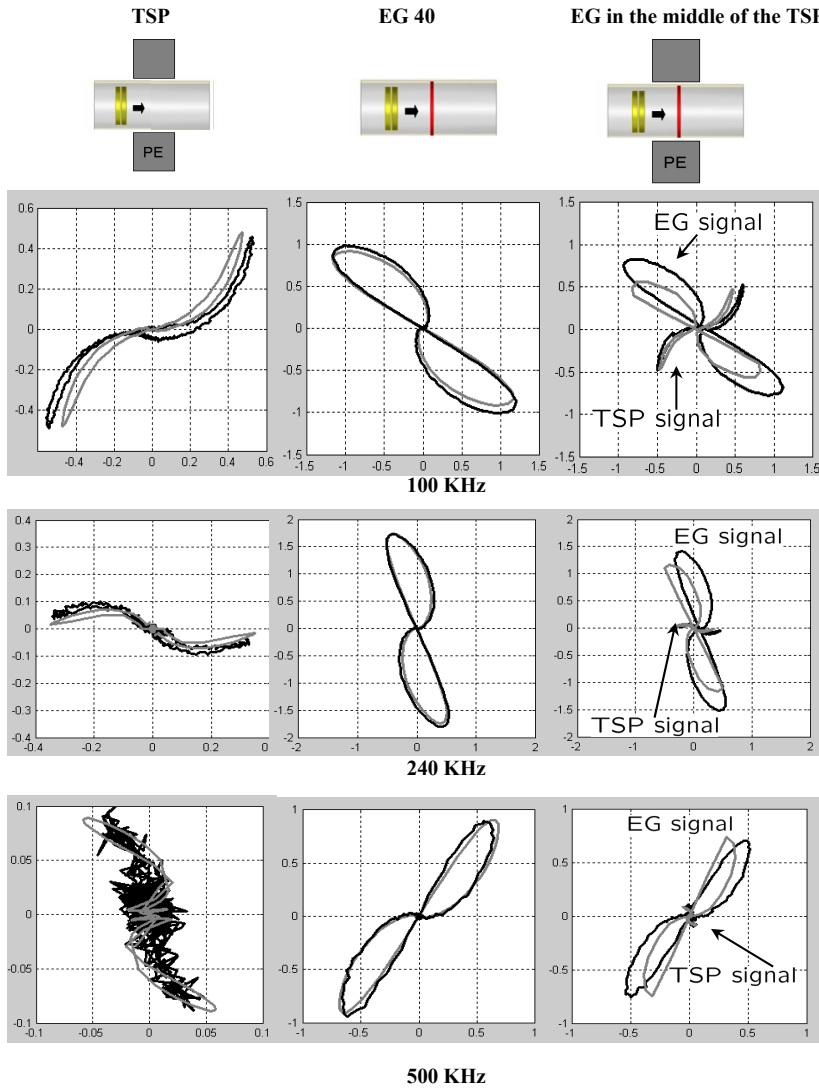


FIGURE 5. Complex plane representation for the signals of the TSP without flaw (left column), the EG40 flaw in the absence of the TSP (central column) and the EG40 flaw in the middle of the TSP at the three measuring frequencies. The grey line represents the simulated signals whereas the black one stands for the measurements. The TSP signals are weaker than the flaw signatures at all frequencies, which allows the safe detection of the latter.

Figure 5 compares the TSP signal in the complex plane with the EG40 flaw signal without the plate and the one obtained by the EG40 when the TSP is present. The defect is centered in respect to the TSP.

The corresponding results for the transversal TT82 and the longitudinal ELN10 notch, at 240 kHz are given in Figure 6. The two defects are axially centered in respect to the TSP and their angular position aligns with the centre of one of the plate's segments.

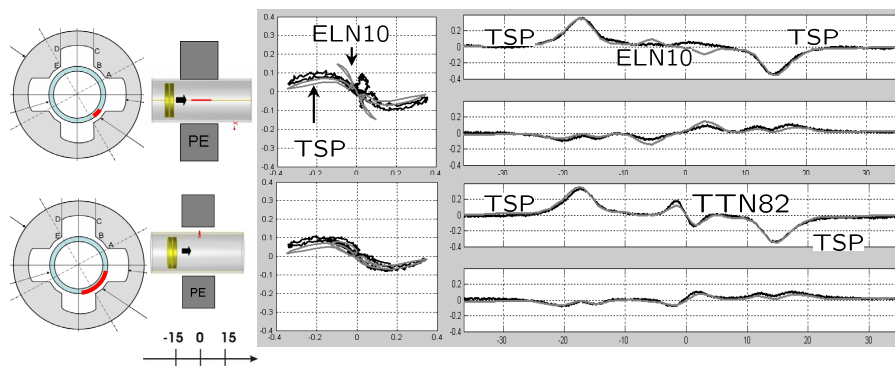


FIGURE 6. Simulated vs. measured signals for two notches at 240 kHz: (a) longitudinal notch (ELN10), and (b) transversal through-notch (TTN82). The above plots give the signals on the complex plane (left side) and their real and imaginary parts as function of the probe scanning position.

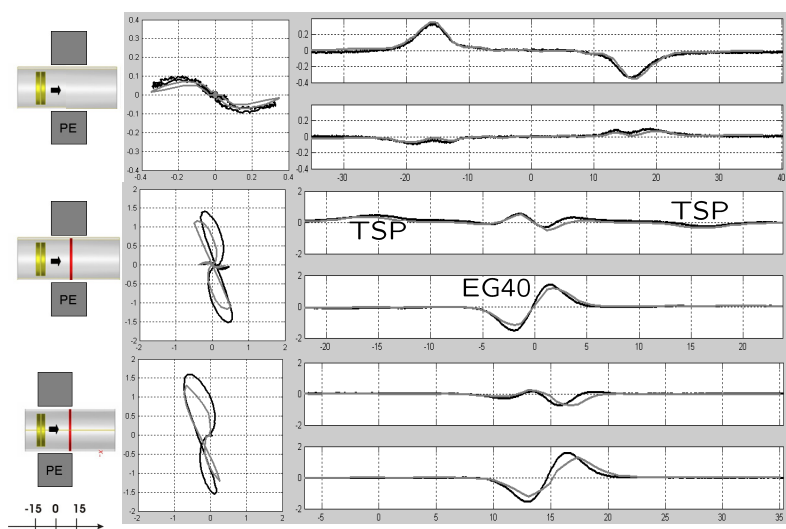


FIGURE 7. Influence of the axial flaw position: (a) signal of the TSP without flaw at 240 kHz, (b) EG40 flaw concentric with the TSP at the same frequency, and (c) EG40 flaw centered on the edge of the TSP. Even if the TSP right signal peak perturbs the flaw signature in the third case, the latter remains distinguishable due to its relative large magnitude in respect to the TSP signal. Again, the plots give the signals on the complex plane (left side) and their real and imaginary parts as function of the probe scanning position.

The effect of the flaw positioning is depicted in Figure 7, where are compared the EG40 flaw signals at 240 kHz for two different axial positions of the latter: once in the middle of the TSP and once centered on the edge of the TSP.

In Figure 8 are compared the calculated signals of the axially non-centered longitudinal notch ELN10, for two different angular locations of the latter: once aligned with the centre of one of the TSP segments and once facing its edge. One can see that the

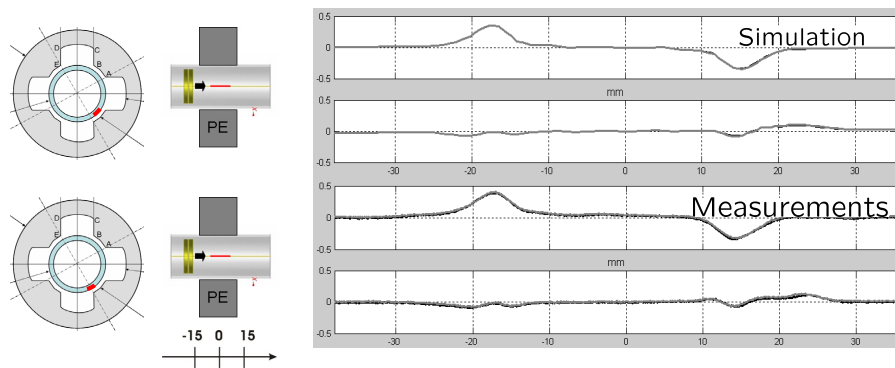


FIGURE 8. Influence of the angular position of the flaw. The two plots correspond to the real and imaginary parts of the signal for a centered longitudinal notch (ELN10) at the angular positions sketched on the mock-up cross-section on the left side. The two curves of the plots almost coincide which shows that the angular position has a negligible influence to the results.

two signals are identical, which means that the angular position of the defect has negligible effects to the final signal. The same results are obtained when comparing the measured signals for the two positions of the defect.

CONCLUSIONS

A hybrid FEM-VIM approach for the simulation of eddy-current inspection of tubes near support plates with quatrefoil TSPs has been presented. Since the primary field is independent of the flaw, the FEM calculations are performed only once for each probe position and each frequency. Different defects can be thus calculated using the same FEM solution for the primary field with an additional computational effort of one VIM-solver call per defect, which running time is of the order of a couple of minutes depending the flaw geometry.

The results of the method are in good agreement with experimental data in all cases. Ferromagnetic TSPs and material deposit in the vicinity of the TSP responsible for clogging up effects will be considered in a next step. Such effects are proved to be directly connected with major SG tube degradations [6] and their accurate modeling is thus of substantial interest. Work is also in progress for the modeling of SG tube inspection in the tubesheet transition zone using surface riding coils.

REFERENCES

1. V. Monebhurrun, D. Lesselier, and B. Duchêne, *J. Electromagn. Waves Appl.* **12**, pp. 315-347 (1998).
2. G. Pichenot, D. Prémel, T. Sollier, and V. Maillot, “Development of a 3D electromagnetic model for eddy current tubing inspection: Application to steam generator tubing”, in *Review of Progress in QNDE*, **16** (2005), pp. 79-100.
3. A. Skarlatos, CG Pascaud, G. Pichenot, G. Cattiaux and T. Sollier, “Modelling of steam generator tubes inspection in the proximity of support plates area via a coupled finite elements – volume integral method approach”, in *Electromagnetic Non-Destructive Evaluation (XII), Studies in Applied Electromagnetics and Mechanics*,

edited by Y. K. Shin, H. B. Lee and S. J. Song, IOS Press, Amsterdam, (2009), pp. 51-58.

4. <http://www-civa.cea.fr>
5. B. A. Auld, "Theoretical characterization and comparison of resonant-probe microwave eddy-current testing with conventional low-frequency eddy-current methods", *Eddy-Current Characterization Material Structures*, edited by G. Birnbaum and G. Free, American Society for Testing and Materials, **12** (1981), pp. 332-347.
6. H. Bodineau and T. Sollier, "Tube support plate clogging up of French PWR steam generators", *Eurosafe*, 2008.